

## Experimental Evaluation of Factors Affecting Tensile Capacity of Connection between Lead Damper and Concrete Foundation

H. Asada<sup>1</sup>, S. Kishiki<sup>2</sup>, and A. Wada<sup>3</sup>

<sup>1</sup>Graduate Student, Tokyo Institute of Technology, Yokohama, Japan

<sup>2</sup>Assistant Professor, Tokyo Institute of Technology, Yokohama, Japan

<sup>3</sup>Professor, Tokyo Institute of Technology, Yokohama, Japan

Email: asada@serc.titech.ac.jp, kishiki@serc.titech.ac.jp, wada@serc.titech.ac.jp

### ABSTRACT :

It has been strongly requested in highly seismic areas to consider not only structural performances but also maintenances of aseismic members in design procedure. Base-isolated structures have both functions to be applied to important buildings. However, brittle fractures at the connections between lead dampers and concrete foundations were observed in 2005 Fukuoka Earthquake. Seismic resistance of damper is transmitted to concrete foundations through the anchor bolts. Therefore, these connections require sufficient stiffness and strength to prevent their deformation and fracture even if dampers are damaged by seismic load. Tensile tests on anchor bolts were conducted to evaluate some factors affecting tensile capacity and failure modes. The main parameters were types of anchor bolts commonly used in anchorage of the lead dampers and layout of reinforcement around the anchor bolt. Based on results of tensile tests, Factors affecting tensile behavior of anchor bolt were discussed.

**KEYWORDS:** Base isolated structure, Connection, Lead damper, Anchor bolt, Tensile capacity, Concrete Cone failure

### 1. INTRODUCTION

Connection between lead damper that is one of the popular damping devices for seismic isolation system and concrete foundation is designed on the premise of replacing damper. These connections also require sufficient stiffness and strength to prevent their own deformation and failure so as to dissipate enough earthquake energy by dampers. When large drift occurs at isolation system, large tensile forces acted on the anchor bolts which connects lead damper to concrete foundation. Brittle fractures caused by tensile forces in connection were observed in 2005 Fukuoka Earthquake.

Lead damper connection types, which are commonly used in Japan, are shown in Figure 1. There are two connection types, stud-type connection and long nut-type connection. In case of the stud-type connection, base plate is anchored to concrete using headed studs. As shown in Figure 1-(a), there are some distances between welding positions of studs and locations of tapping holes for attaching lead damper. Therefore, prying actions are caused by deformation of base plate. On the other hand, in case of long nut-type connection shown in Figure 1-(b), headed bolts are connected with bolts for attaching lead damper through the long nut. One example of concrete foundation is shown in Figure 2. Lead damper is installed on the concrete foundation such as "plinth". Note that there are two types of reinforcement around anchor bolts. One is vertical reinforcement to anchor bolts and the other is horizontal reinforcement to anchor bolts in "plinth".

In this study, focusing on these characteristics of connections, tensile tests of anchor bolts were conducted to evaluate factors affecting tensile capacity of anchor bolt.

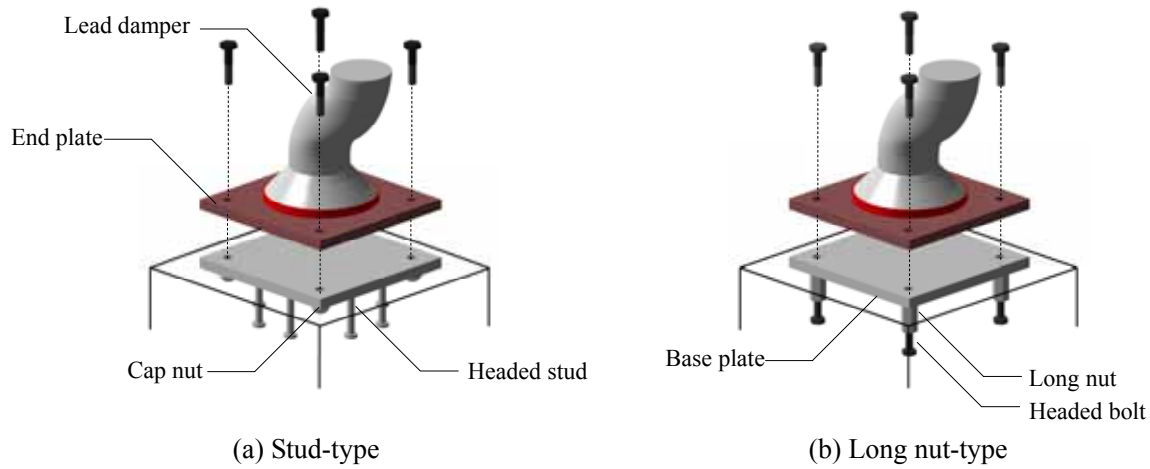


Figure 1 Connection type of lead damper

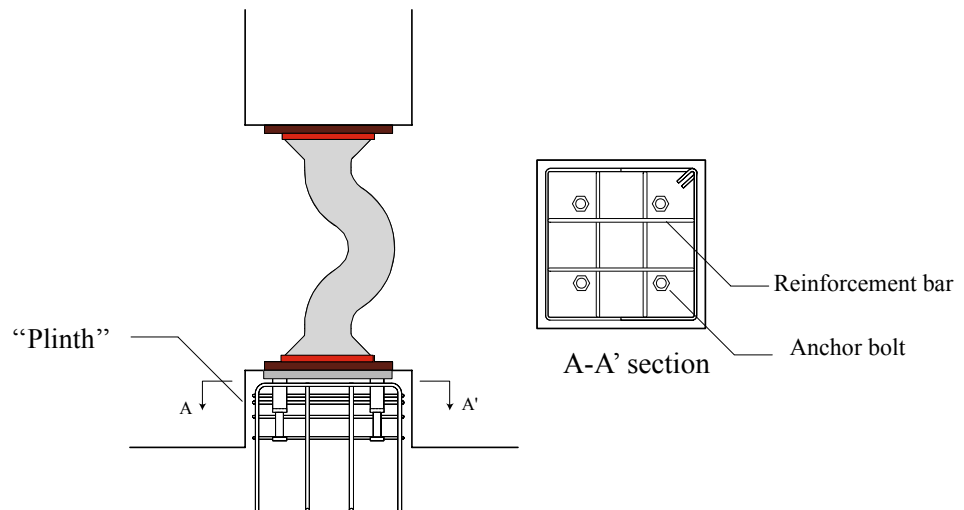


Figure 2 Example of lead damper connection

## 2. TEST PROGRAM

### 2.1. Test specimens

To evaluate effect of types of anchor bolt and reinforcement pattern on tensile behavior of anchor bolts, two test series were selected and were performed 17 specimens in total. Test program is summarized in Table 1. Test series C was focused on the shape of anchor bolts. Test series R was focused on the reinforcement pattern around anchor bolt. Details of anchor bolt are shown in Figure 3. C series specimens are used two different anchor type, one is with headed stud and the other was with headed bolts covered with long nut. However, Specimen C-4 was with headed bolt which was not covered with long nut. The effective embedment depth ( $L_e$ ) was 90mm and 120mm. The length of long nut ( $d_n$ ) was 50, 80, and 100. If the specimen name has last characters UB, the specimen was used headed bolt with unbonded thread portion by taping and greasing. R series specimens were divided into three type depending on arrangement of reinforcement (D13) around anchor bolt as shown in Figure 4. One is reinforced with vertical reinforcement around anchor bolt. The second is reinforced with horizontal reinforcement. The third is reinforced with both vertical and horizontal reinforcement.

The Configuration of test specimen C-2 is shown in figure 6. The size of concrete block was same for all specimens. The size of test block was large enough to neglect the effect of distance from free edges. All specimens were reinforced to the bottom part of the concrete block with  $\cap$ -shaped reinforcements to attach the concrete block to reaction floor through the rigid jig. These reinforcements do not significantly influence the failure. The actual concrete strength at the time of testing is shown in Table 2. The concrete for the all specimen was placed from one batch. Table 3 shows that the material properties of reinforcement and headed studs.

**2.2. Loading method and Measurements**

The test setup is shown in figure 7. The bottom of specimen was fixed to the reaction floor with rigid jig considering actual boundary condition of lead damper connection. Tensile load was applied to the anchor bolt through the PC bar under displacement control at the rate of 0.2 mm per minute. The applied load was measured by load cell embedded in testing machine. Additionally, strain of the anchor bolt and reinforcements around anchor bolt were measured. Furthermore, the displacement of the top end of Anchor bolt was measured by a couple of displacement transducers.

Table 1 Test specimens

Series	Specimen	Type of Anchor bolt	$L_e$ [mm]	$l_n$ [mm]	Arrangement of Reinforcement around anchor bolt			Plate thickness [mm]
					cover thickness $c$ [mm] <sup>*2)</sup>	the number of vert.reinforcement	the number of hori.reinforcement	
C	C-1	headed stud	90	-	-	-	-	-
	C-2	$\phi 19$	120	0				
	C-3	headed bolt hexagon head screw M20 (F8.8T)		50				
	C-4			80				
	C-4UB			100				
	C-5							
	C-5UB							
C-6								
R	R-1	headed stud $\phi 19$	120	-	30	-	2	-
	R-2						4	
	R-2NC <sup>(1*)</sup>							
	R-3						4	
	R-4				60			
	R-5				120			
	R-6				30			
	R-7				60	2	2	
R-8	30	4	4					

\*1 R-2NC was without orthogonal bar show in Fig 4 (a)

\*2 Cover thickness means distance from top surface of concrete block to top face of reinforcement.

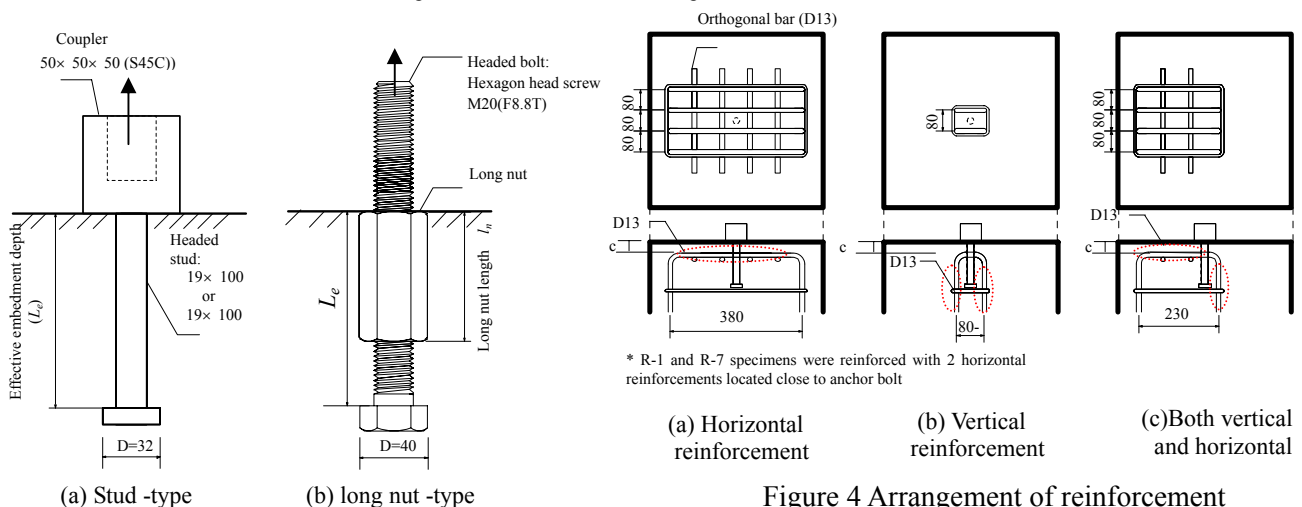


Figure 3 Details of anchor bolts

Figure 4 Arrangement of reinforcement around anchor bolt unit:mm

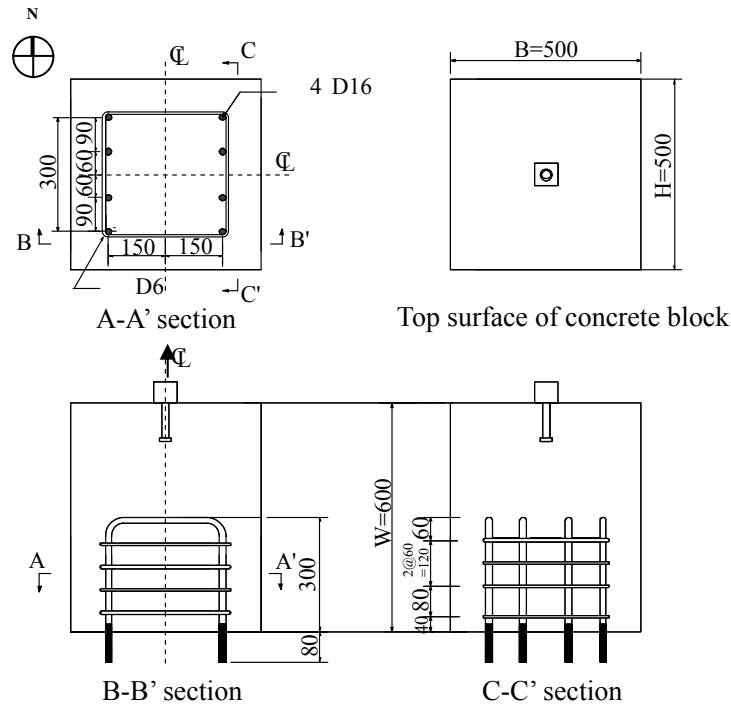


Figure 6 Configuration of specimen C-1 unit:mm

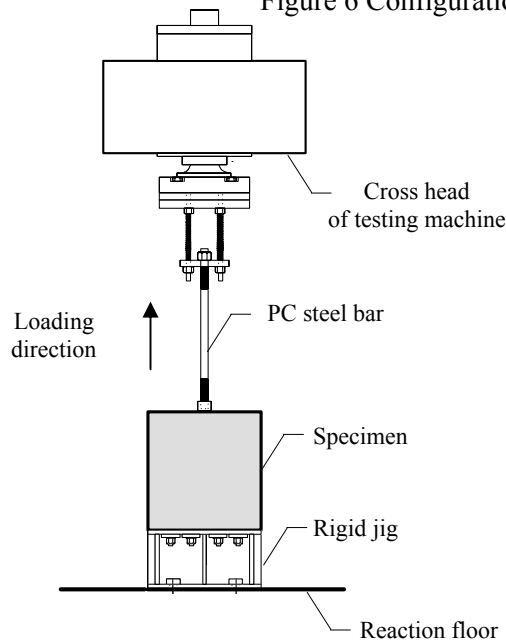


Figure 7 Test setup

Table 2 Concrete strength at the time of testing

series	Tensile strength $f_t$ [N/mm <sup>2</sup> ]	Compressive Strength $f_c$ [N/mm <sup>2</sup> ]	Elastic Modulus $E_c$ [N/mm <sup>2</sup> ]
C series	2.34	27.80	$2.35 \times 10^4$
R series	2.36	29.3	$2.66 \times 10^4$
L series	2.53	30.5	$2.68 \times 10^4$

Table 3 Mechanical properties of reinforcement

	Yield Strength [N/mm <sup>2</sup> ]	Ultimate Strength [N/mm <sup>2</sup> ]	Elastic Modulus [N/mm <sup>2</sup> ]
D6(SD295A)	370	552	$1.87 \times 10^5$
D13(SD295A)	368	521	$1.73 \times 10^5$

Headed stud:  $\sigma_y=407$ [N/mm<sup>2</sup>],  $\sigma_u=457$ [N/mm<sup>2</sup>],

Headed bolt(threaded screw):  $\sigma_y=640$ [N/mm<sup>2</sup>] (nominal yield strength)

### 3. TEST RESULTS AND DISCUSSION

#### 3.1. Failure loads and Failure modes

The test results are summarized in Table 5. Diagrams of failure modes observed in the present tests are shown in Figure 8. In test series C except specimen C-6, finally, failures of specimens were caused by forming of concrete cone. Tensile capacities of stud-type specimens were larger than those of long nut-type specimens relatively. Measured failure loads of long nut-type specimens except specimen C-6 agree well with predicted capacity according to AIJ standard (AIJ 1985) based on the 45-degree cone method. On the other hand, tensile capacity of specimen C-6 was slightly smaller than the predicted capacity because failure of this specimen was

caused by slipping anchor bolt (pull-out) due to the lack of bearing resistance by the anchor head. This was because about 80% of effective embedment depth was covered with long nut. Capacities of reinforced specimens which are placed into R series were larger than predicted capacity. Specially, it should be noted that specimens R-6 and R-7 reinforced with vertical reinforcements are much larger than predicted capacity. As the result, both these specimens were failed by the fracture of anchor steel. Tensile capacities of specimens R-2, R-3 and R-4 with horizontal reinforcements were not significantly increased by the existence of reinforcement. On the other hand, the measured failure load of specimen R-4 with horizontal reinforcements which arranged 120mm from the top surface of the concrete block was approximately 10% lower than that of unreinforced specimen C-2. From the shape of the concrete cone failure, it seems that these horizontal reinforcements help to form the concrete failure. Typical shape of concrete cone failure surface is shown in Figure 9. The depth of failure surface was measured by laser displacement sensor after removal of broke piece of concrete block. In Figure 10, A-A' sections of failure surface and failure surface idealized according to AIJ were illustrated. the slope of the concrete cone was much flatter than 45 degree assuming in design procedure, regardless of the embedment depth, anchor type and reinforcement pattern. The slope angle of cone for unreinforced specimens varied from  $\theta=15$  to 25 degrees.

Table 5 Test results

Test Series	Specimen	$exp. P_u^{1*)}$ [kN]	$cal. P_u^{2*)}$ [kN]	Failure mode <sup>3*)</sup>	$exp. P_u / cal. P_u$
C	C-1	75.46	57.90	C	1.30
	C-2	113.68	96.19	C	1.18
	C-3	93.70	99.82	C	0.94
	C-4	99.26		C	0.99
	C-4UB	103.73		C	1.04
	C-5	108.06		C	1.08
C-5UB	101.35	C		1.02	
C-6	91.38	S		0.92	
R	R-1	115.83	96.19	C	1.20
	R-2	121.09		C	1.26
	R-2NC	109.72		C	1.14
	R-3	114.32		C	1.19
	R-4	102.45		C	1.07
	R-5	132.41		F	1.38
	R-6	129.79		F	1.35
	R-7	128.38		C	1.33
R-8	133.63	F	1.39		

\*1  $exp. P_u$ : measured tensile capacity

\*2  $cal. P_u$ : predicted concrete cone capacity according to AIJ<sup>2)</sup>

$$cal P_u = -0.31 \sqrt{F_c} * A_c [N] \quad (\text{SI equivalent})$$

with  
 $A_c$  = projected area  
 $= \pi L_e (L_e + D)$

\*3 Failure Mode: C: Concrete cone failure,  
 S: Slip failure (Pull-out failure),  
 F: Steel failure

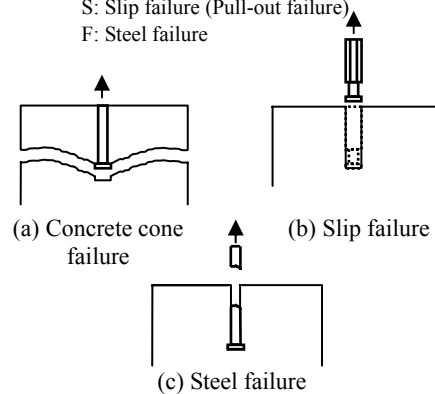


Figure 8 Diagrams of Failure modes

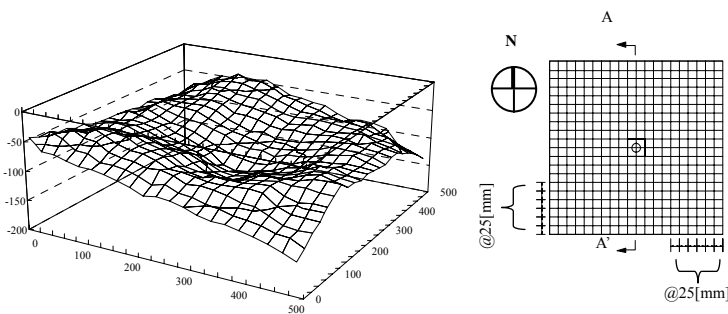


Figure 9 Typical shape of concrete cone failure surface

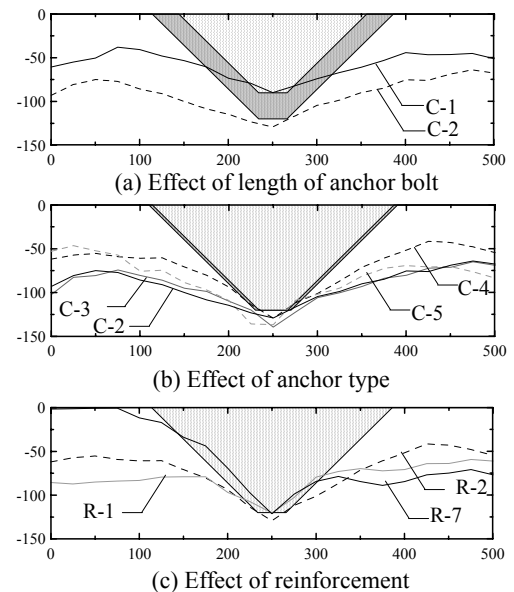


Figure 10 A-A' section of failure surface

### 3.2. Feature of Tensile Deformation Behavior for long nut-type specimen

Tensile load-tensile deformation curves for long nut-type specimens with threaded portion and with unbonded threaded portion are shown in Figure 11. Tensile deformation includes steel elongation of anchor length. Tensile capacities of specimens with bonded threaded portion and those of specimen with unbonded threaded portion were almost same. However, tensile deformations of specimens with bonded threaded portion were more than twice those of specimens with unbonded threaded portion at the peak load of each specimen. As show in Figure 12, the linear relation between the tensile deformation of long nut-type specimens excepts specimen C-6 (which was failed by slipping anchor) at the peak load and ‘‘long nut coverage’’  $\alpha$  defined by equation (3.1) was observed. In case of long nut-type, it can be concluded that the bond resistance by threaded portion have potent influence on tensile deformation behavior. And also in design procedure, length of long nut should be treated with enough care because tensile capacity may decreases by occurring slip failure if most of embedment length was covered with long nut.

### 3.3. Contributory Effect of reinforcement to tensile capacity

In Figure 13, bending moment distribution obtained from the measured strains of horizontal reinforcement in specimen R-2 is plotted. Maximum average shear force between measuring points was 0.05 kN. That is, resistance caused by dowel action of horizontal reinforcement to tensile load was extremely low. Measured tensile load versus axial force acting on vertical reinforcement obtained from the measured strain for specimen R-5 is shown in Figure 14. At the 70% of peak load, the percentage of the sum of axial force acting on vertical reinforcements was only 7.5% of tensile load. Meanwhile, at the peak load, the percentage of the sum of axial force acting on vertical reinforcements was 22% of tensile load. The results indicate that vertical reinforcement contributes to redundancy of tensile capacity.

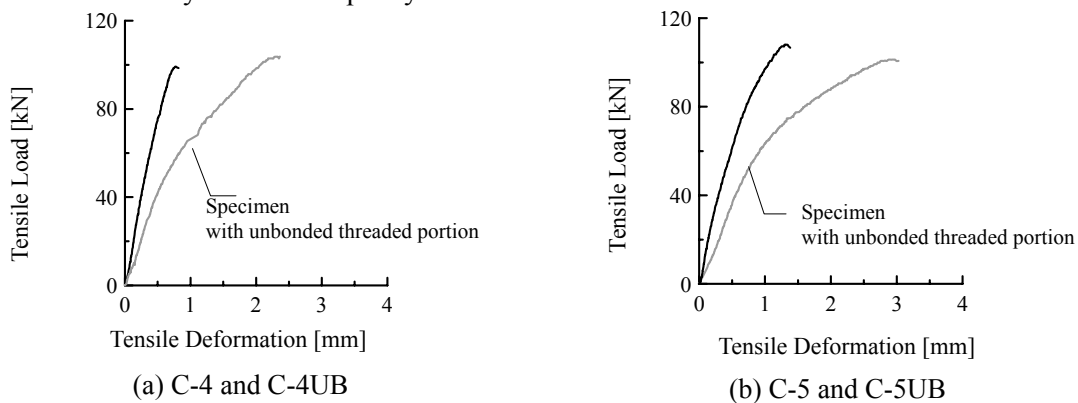


Figure 11 Load-deformation curves for long nut type specimen with threaded portion and with unbonded threaded portion

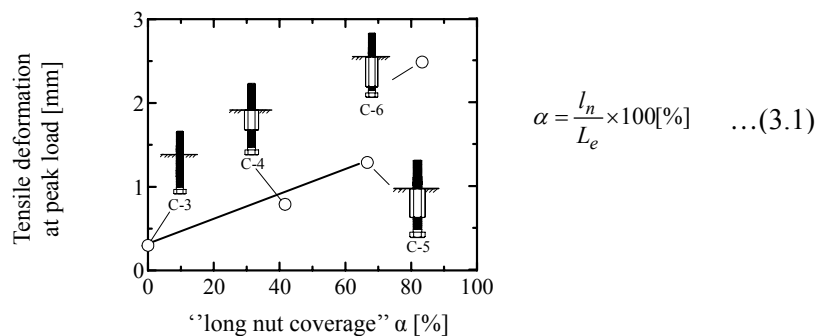


Figure 12 Comparison of tensile displacement at peak load for long nut-type specimens

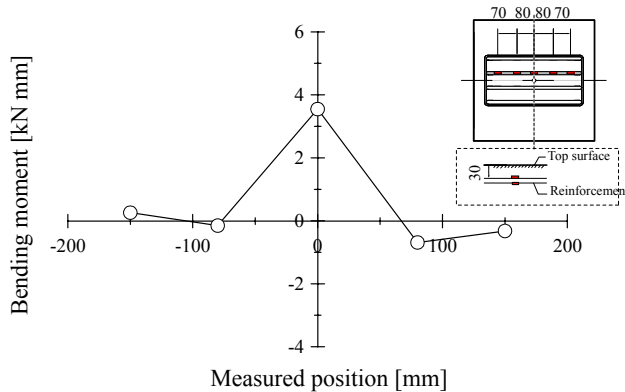


Figure 13 Bending moment distribution acting on horizontal reinforcement at peak load for R-2

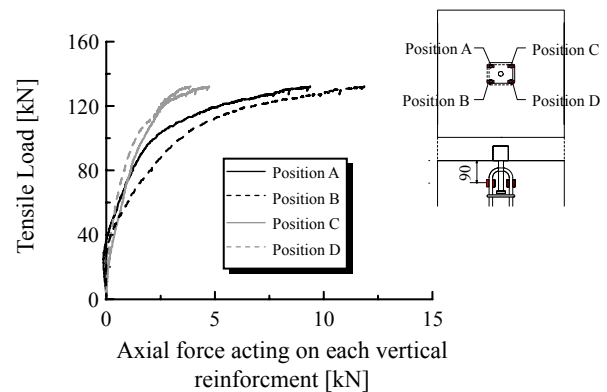


Figure 14 Measured tensile load versus axial force acting on vertical reinforcement for R-5

### 3.4. Observation about Effective projected area of concrete cone surface

As shown in Figure 9, observed cone failure covered whole area of top surface of concrete block. Quasi-tensile force obtain from multiplying concrete tensile strength obtain from cleave test by measured failure surface area, was much larger than measured tensile capacity of concrete cone failure. For this reason, it is assumed that surface area of cone with radius  $\beta L_e$  resist the tensile force  $P$  as shown in Figure 15. Other assumption to calculate tensile capacity using concrete resistance model as shown in Figure 15 are below.

- (1) Failure surface is axisymmetric.
- (2) When failure occurs, Maximum principal stress acts in vertical to failure surface.
- (3) When maximum principal stress reach concrete tensile strength obtained from cleave test, failure occurs.
- (4) Stress distribution on failure surface is uniform.

Based on these assumptions, the concrete capacity can be calculated by Equation (3.2)

$$P_u = 2\pi \int_{D/2}^{\beta L_e + D/2} (f_t \cos \theta) \cdot \frac{r}{\cos \theta} dr = f_t \pi \beta L_e (\beta L_e + D) \quad \dots(3.2)$$

Where

- $f_t$  = concrete tensile strength, N/mm<sup>2</sup>
- $\theta$  = angle of failure surface, rad
- $D$  = head diameter of headed stud or headed bolt, mm
- $L_e$  = effective embedment depth, mm

According to Equation (3.2), Concrete cone capacity is governed by horizontal effective projected area and tensile capacity of concrete, despite angle of concrete cone. In Table 6, each  $\beta$  calculated back with measured tensile capacities of specimens of C series, whose failures were concrete cone failure, are given. From results of present tests, Radius of effective projected area  $\beta L_e$  was  $0.81L_e - 0.96L_e$ . Substituting  $f_t$  with  $0.31\sqrt{F_c}$  (In engineering unit  $f_t = \sqrt{F_c}$ ) and  $\beta$  into 1.0, Equation (3.2) corresponds to design formula of Japanese design provision (AIJ).based on 45-degree cone model. It is concluded that the projected radius of effective failure surface estimated at  $0.81L_e - 0.96L_e$  give close agreement with radius of effective failure surface idealized according to AIJ.

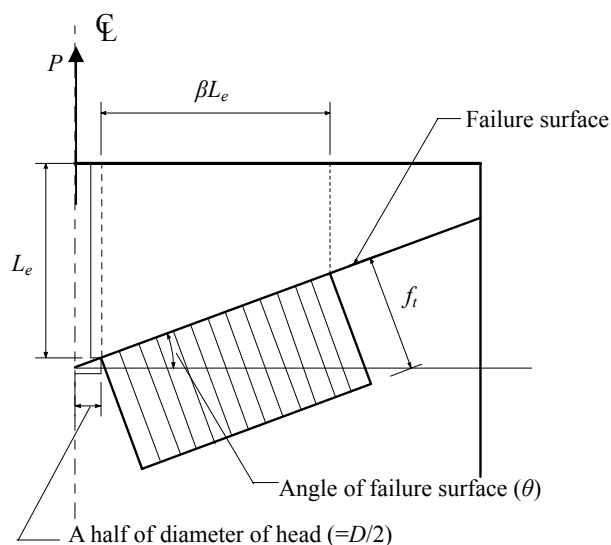


Table 6 Value of  $\beta$  for each specimen

specimen	$\beta$
C-1	0.96
C-2	0.91
C-3	0.82
C-4	0.81
C-4UB	0.84
C-5	0.86
C-5UB	0.82
Mean Value	0.86

Figure 16 Stress distribution when failure occurs  
 (Concrete resistance model)

#### 4. CONCLUSION

In this study, in order to evaluate factors affecting tensile behavior of connection between lead damper and concrete foundation, tensile tests of anchor bolt which connect lead damper to concrete foundation, were conducted. The following conclusion can be drawn based on the test results and discussion.

1. From results of tensile test considering actual boundary condition of lead damper connection, The slope of the concrete cone was much flatter than 45 degree assuming in design procedure, regardless of the embedment depth, anchor type and reinforcement pattern. For unreinforced specimens, the slope angle of cone with concrete surface varied from  $\theta=15$  to 25 degrees.
2. In case of long nut-type, the bond resistance by threaded portion has potent influence on tensile deformation behavior. Tensile capacity of specimen C-6 whose approximately 80% of effective embedment depth was covered with long nut, was smaller than the predicted capacity because failure of this specimen was caused by slipping anchor bolt.
3. Vertical reinforcements around anchor bolt contribute to redundancy of tensile capacity.
4. Using simple concrete resistance model, Effective radius of projected area were assessed  $0.81L_e - 0.96L_e$ . These values were close to effective radius  $1.0 L_e$  in existing design formula according to AIJ.

#### ACKNOWLEDGEMENTS

This study was supported by a grant from Japan Society of Seismic Isolation and The Building Center of Japan. The authors would like to express our appreciation to companies.

#### REFERENCES

- Takayama, M., Morita, K., Kashiwagi, E., and Ando, M. (2006) . Experimental Study on the Axial Force and the Bending Moment of U180 Type Lead Damper Part 1 and 2. Proceedings of annual meeting of Architectural Institute of Japan, **B-2: 617-620** (in Japanese).
- Architectural Institute of Japan (AIJ). (1985). Design Recommendations for Composite Constructions. (in Japanese)